Real Linear Automata with a Continuum of Periodic Solutions for Every Period

XU, Xu <http://orcid.org/0000-0002-9721-9054>

International Journal of Bifurcation and Chaos

Real Linear Automata with a Continuum of Periodic Solutions for Every Period

Xu Xu[1,2]
[1] *Department of Engineering and Mathematics,*
[2] *Materials & Engineering Research Institute,*
Sheffield Hallam University, Sheffield, S1 1WB (UK)
Xu.Xu@shu.ac.uk

Received (to be inserted by publisher)

Interesting dynamical features such as periodic solutions of binary cellular automata are rare and therefore difficult to find, in general. In this paper, we illustrate an effective method in identifying fixed and periodic points of traditional one- and two- dimensional p-valued cellular automaton systems, using cycle graphs. We also show when the binary or p-valued cellular states are extended to real-values and when defined as doubly-infinite vectors, there exists a continuum of periodic solutions for every period, even when the governing local rules are simply linear. In addition, we demonstrate the important effect boundary conditions have on systems' dynamical structures.

Keywords: real-valued cellular automata; discrete nonlinear dynamics; linear rules; equilibria; periodic solutions; boundary conditions.

1. Introduction

The field of cellular automata (CA) has generated a vast amount of interest, since its creation by von Neumann in the 1940s [Von Neumann *et al.*, 1966]. This was further boosted by Wolfram's remarkable numerical experiments conducted from the 1980s ([Wolfram, 2018] and [Wolfram, 1984]) and by a series of ground-breaking nonlinear dynamics studies from Chua and co-researchers in the early 21st century ([Chua *et al.*, 2002], [Chua *et al.*, 2003] [Chua *et al.*, 2004], [Chua *et al.*, 2005a], [Chua *et al.*, 2005b], [Chua *et al.*, 2006], [Chua *et al.*, 2007a], [Chua *et al.*, 2007b] and [Chua *et al.*, 2008]).

People are fascinated by CA, because in these systems, amazingly complex patterns and dynamical behaviours emerge when governed by very simple locally interacting rules. Apart from the ones mentioned earlier, many other researchers have also contributed to the theoretical, analytical and computational understanding of CA. For example, Voorhees performed computational analysis on 1D binary CA [Voorhees, 1996]. Jen analysed enumeration of preimages which provided CA rule's probability distribution information [Jen, 1989]. Ilachinski systematically explored features and applications of CA, particularly in information-based discrete physics [Ilachinski, 2001]. Chopard and his collaborators investigated a variety of CA applications, especially in studying microscopic fluid dynamics and particle transport when linked with the lattice Boltzmann technique [Chopard & Masselot, 1999],[Chopard *et al.*, 2002], [Chopard, 2012]. The hybrid CA and lattice gas method was originally introduced by Frisch, Hasslacher and Pomeau in [Frisch *et al.*, 1986] as a discrete Navier-Stokes equation solver obeying mass and momentum conservations, and Wolf-Gladrow gave a comprehensive description of its concept and recent development into the

lattice Boltzmann models in [Wolf-Gladrow, 2004].

Furthermore, CA have also been studied as spatially and temporally discrete nonlinear dynamical systems. In our previous work [Xu *et al.*, 2009], we classified one-dimensional (1D) binary CA based on Smale's basic sets and nonwandering points as well as introducing mathematical and numerical techniques for identifying periodic points and basic sets. These share a common perspective as Mainzer and Chua's work [Mainzer & Chua, 2011] and many of the results agree. Wuensche and co-researcher studied global dynamics, in particular, the basins of attraction, of 1D binary CA systems ([Wuensche & Lesser, 1992], [Wuensche, 1992], [Wuensche, 2000] and [Wuensche, 2017]. Martinez summarised several classifications of elementary CA in [Martinez, 2013]. Uguz and collaborators investigated the effect the underlying lattice grid has on the CA dynamics in [Uguz *et al.*, 2013] and [Uguz *et al.*, 2017], and linear two-dimensional (2D) CA over ternary field [Sahin *et al.*, 2015]. The de Bruijn graph, an alternative representation of the local rule table, can be used to determine fixed points and the reversibility of 1D CA ([Sutner, 1991], [Bhattacharjee *et al.*, 2018], [Martínez *et al.*, 2018], [McIntosh, 1991] and [McIntosh, 2009]). This method was extended into 2D to compute the well-known Conways game of Life CA in [McIntosh, 2010].

As mentioned earlier, CA do not only create complex and interesting dynamical structures, but have also shown surprising ability to reproduce complex behaviours observed in real systems. Therefore, they have a very wide range of applications, when used as a mathematical framework and a computational tool for modelling. These include:

(i). biological models of life processes, e.g. ant colonies [Chopard & Droz, 1998], [Bossomaier & Green, 2000] and bird flocking [Ermentrout *et al.*, 1993];

(ii). ecological and geological models, e.g. forest fire [Karafyllidis & Thanailakis, 1997], forest insect disturbance [Perez & Dragicevic, 2012] and fast moving landslides [Avolio *et al.*, 2013];

(iii). social and behavioural models: eg. residential migration [Dabbaghian *et al.*, 2010], urban growths [Liu *et al.*, 2017], evacuation process, traffic flow and pedestrian dynamics, etc.;

(iv). micro-structure of material process models, eg. austenite grain growth and coarsening [Vertyagina *et al.*, 2013] [Zhu *et al.*, 2014],[Raabe, 2002], [Han *et al.*, 2015], [Vertyagina & Mahfouf, 2015], [Wang *et al.*, 2017], alloy solidification [Zhao *et al.*, 2013] and shape rolling [Svyetlichnyy, 2012], additive manufacturing [Rai *et al.*, 2016] etc.;

(v). micro-biological modelling, e.g. tumour growth [Al-Husari *et al.*, 2014], response of a solid tumour to chemotherapy [Powathil *et al.*, 2012], influenza A viral infections [Beauchemin *et al.*, 2005], hepatitis B viral infections [Xiao *et al.*, 2006] and ebola virus dynamics [Burkhead & Hawkins, 2015] etc.

The concept of CA has also been applied in producing powerful chaotic image encryption programmes [Machicao *et al.*, 2012] and [Ping *et al.*, 2014].

Most of the CA models used binary or boolean elements in their states, which rather limited their modelling accuracy and efficiency. The binary variables can be extended to p-values (where p is an integer) and then to real-values, to offer more flexibility and versatility. The various types of CA were shown in a comprehensive recent survey by Bhattacharjee and co-researchers [Bhattacharjee *et al.*, 2016]. The real-valued CA, unsurprisingly, generate an even richer amount of structures such as fractal, chaotic and hypercyclic [Bayart & Matheron, 2009], which we explored in [Xu *et al.*, 2011]. This previous work laid solid foundation for theoretical understanding of cellular systems with real-valued states as well as facilitating more realistic modelling approaches for real systems. It also paved a path for the results and analysis demonstrated in this paper.

This paper is organised as follows: in Sec. 2, we present a cycle graph method, similar to the de Bruijn graph but simpler in its format, for obtaining periodic points of one- and two- dimensional p-valued cellular systems. The later four sections focus on real-valued CA. More specifically, in Sec. 3, we analyse equilibria and periodic solutions of one-dimensional CA with different restrictive boundary conditions. When these boundary conditions are lifted, we show in Sec. 4 and Sec. 5, that there exist a rich set of periodic solutions for every period.

2. Periodic Solutions of Discrete Cellular Systems

Before considering the case of real-valued cellular systems, we shall first examine the case of discrete p-valued systems. For simplicity we shall begin with systems having doubly-infinite state

$$\mathbf{x} = \cdots x_{-1}x_0x_1\cdots,$$

where $x_i \in \{0, 1, \cdots, p-1\}$, $-\infty < i < \infty$.

Thus,

$$\mathbf{x} \in \prod_{-\infty<i<\infty} \{0, 1, \cdots, p-1\} = \{0, 1, \cdots, p-1\}^{\mathbb{Z}}.$$

The dynamics are given by

$$\mathbf{y} = F(\mathbf{x}),$$

where

$$y_i = (F(\mathbf{x}))_i = f(x_{i-q}, \cdots, x_i, \cdots, x_{i+q}) \tag{1}$$

for some positive integer q. (For a simple three-bit binary automaton, $p = 2$, $q = 1$ and the 'length' of the neighbourhood is $2q + 1$.) Note that , if we apply F twice, then

$$\mathbf{y} = F^2(\mathbf{x}),$$

where

$$y_i = f(z_{i-q}, \cdots, z_i, \cdots, z_{i+q})$$

and

$$z_j = f(x_{j-q}, \cdots, x_j, \cdots, x_{j+q}), \quad i - q \le j \le i + q.$$

Hence F^2 is equivalent to a system with neighbourhood length $4q + 1$ [Xu *et al.*, 2009]. It follows that, in order to study periodic solutions of period m, we can consider the fixed points of an equivalent system F^m with neighbourhood length $2mq + 1$. Therefore we need to consider only fixed points of general systems with an arbitrary neighbourhood.

In order to specify the system, we must define the function f in (1). It is a discrete function depending on $2q + 1$ variables, each having p values and the range of the function also having p values. For small values of p and q, we usually specify f in the form of a table; for example, for a binary, 3-bit rule (Rule 126), we may define

Table 1. A binary 3-bit function Example.

	f
000	0
001	1
010	1
011	1
100	1
101	1
110	1
111	0

giving rise to Sierpinski-type dynamics (which could also be generated by Rule 90 and several other rules). In the case of large p and / or q, such a table becomes impractical (there are $p^{(2q+1)}$ lines in the table). However, for the purpose of studying fixed points, we shall see that we only need a 'partial table' – namely, only those lines of the table in which the central digit on the left is the same as the right (the output). Thus, in Table 1, we have

Table 2. A binary 3-bit partial table.

	f
000	0
010	1
011	1
110	1

From (1), this is just the relation

$$x_i = f(x_{i-q}, \cdots, x_i, \cdots, x_{i+q}). \tag{2}$$

For systems with large p and / or q, if the number of values of $(x_{i-q}, \cdots, x_i, \cdots, x_{i+q})$ is bounded by some number N for which the tabulation of solutions if (2) is possible, then the method will be feasible.

We now associate a directed graph with the relation (2). The vertices of the graph are the values of $(x_{i-q}, \cdots, x_i, \cdots, x_{i+q})$ which satisfy (2). If there are N solutions of (2), we will denote them by $v_1, \cdots, v_N$. Thus, for each $j \in \{1, \cdots, N\}$, there exist $\xi^j_{-q}, \cdots, \xi^j_0, \cdots, \xi^j_q$, such that

$$v_j = \left(\xi^j_{-q}, \cdots, \xi^j_0, \cdots, \xi^j_q\right)$$

and

$$\xi^j_0 = f(v_j) = \left(\xi^j_{-q}, \cdots, \xi^j_0, \cdots, \xi^j_q\right).$$

For example, in Table 2, we have

$$\begin{aligned} v_1 &= (000), \\ v_2 &= (010), \\ v_3 &= (011), \\ v_4 &= (110). \end{aligned} \tag{3}$$

The graph has a directed edge from v_j to v_k if the vectors corresponding to v_j and v_k 'fit together' in the sense that, if

$$v_j = \left(\xi^j_{-q}, \cdots, \xi^j_0, \cdots, \xi^j_q\right),\ v_k = \left(\xi^k_{-q}, \cdots, \xi^k_0, \cdots, \xi^k_q\right)$$

then

$$\xi^j_{(-q+l)} = \xi^k_{(-q+l-1)},\ 1 \le l \le 2q.$$

We shall write such a directed edge by $e_{jk} = (v_j, v_k)$. Thus in the case of (3), we have the directed edges

$$e_{11} = (v_1, v_1),\ e_{34} = (v_3, v_4),$$

giving the directed graph shown in Fig. 1.

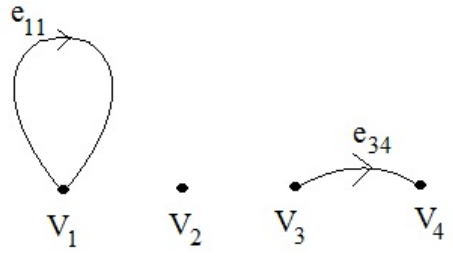

Fig. 1. Directed graph of the system defined by Table 2.

The following result now follows from the above remarks: Consider a q-bit, p-valued one-dimensional cellular automaton given by the function (1). Let G be the graph related to the rule as above. Then the automaton has a fixed point if and only if G has a cycle.

Note, the 1D cycle graph presented here is similar to the de Bruijn graph [Sutner, 1991] (traditionally used for the analysis of 1D CA [Bhattacharjee *et al.*, 2016]), but it is a partial graph which only contains vertices that have the central digit of the input fixed at the output from the rule table, therefore it is simpler in its format. The main advantage of the new cycle graph is that it can be easily extended to identify periodic solutions of higher periods for 1D CA and fixed points for 2D CA, because of this simplicity. Next, we shall show examples of period-2 and period-5 solutions for 1D CA Rule 82 to further explain this point.

Example 2.1. Consider the 1D binary CA governed by the 3-bit rule as shown in Table 3.

Table 3. 1D 3-bit CA Rule 82

	f
000	0
001	1
010	0
011	0
100	1
101	0
110	1
111	0

In order to find period-2 orbits of this 3-bit CA system, we consider the fixed points of the corresponding system F^2, with a neighbourhood length 5 ($2mq+1 = 2\times 2\times 1+1$), of which the updated 5-bit rule table is given in Table 4, with 32 (2^5) lines.

Table 4. 1D 5-bit CA Rule, corresponding to the 3-bit CA Rule 82

	f		f		f		f
00000	0	01000	0	10000	1	11000	1
00001	1	01001	0	10001	0	11001	0
00010	0	01010	0	10010	1	11010	1
00011	0	01011	0	10011	1	11011	1
00100	0	01100	0	10100	1	11100	0
00101	1	01101	0	10101	0	11101	0
00110	0	01110	1	10110	1	11110	1
00111	1	01111	0	10111	0	11111	0

Within the 32 configurations from Table 4, 15 of them satisfy the relation defined in Eq. (2) (i.e they have the central digit fixed). These form vertices of a partial rule graph and together with the directed edges linking vertices which fit together, we obtain a directed graph for this 5-bit system shown in Fig. 2. Cycles in this graph represent fixed points of the 5-bit CA which are in fact period-2 points of the 3-bit CA Rule 82.

In order to better visualise the cycles, Fig. 2 can be simplified by showing the vertices and edges which are part of a cycle only (removing all vertices and edges which do not belong to any cycle), as shown in Fig. 3. The fixed points of the 5-bit CA defined by Table 4, which are periodic solutions of period-2 for the 3-bit CA Rule 82 defined in Table 3, can now be easily read out from Fig. 3. For example, 001010 (complete the cycle following the sequence of vertices: 3, 5, 7, 4, 6, 2) when subject to periodic boundary conditions, is a period-2 point.

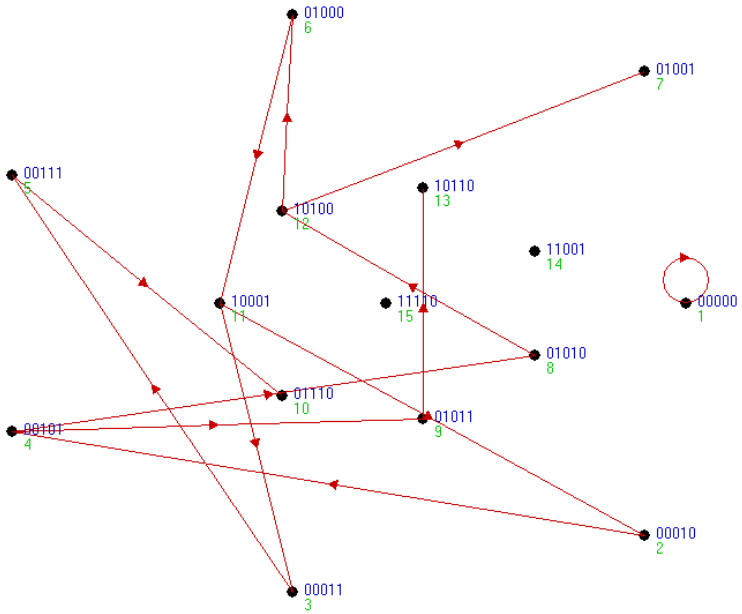

Fig. 2. Directed graph of the system defined by Table 4.

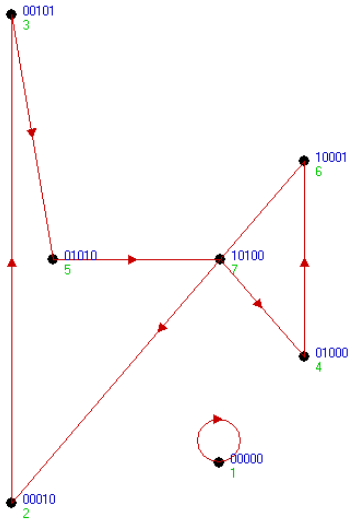

Fig. 3. Simplified directed graph from Fig. 2.

Periodic points of higher periods can also be identified using the cycle graph method, but we will expect to see more complicated graphs. For example, the period-5 points of the 3-bit CA Rule 82 correspond to fixed points of a new system F^5, with a neighbourhood length 11 ($2mq+1 = 2\times 5\times 1+1$). The rule table has 2048 (2^{11}) lines and therefore is not practical to be presented here. However, following the same steps as the period-2 case shown earlier, we plot the directed graph of this 11-bit CA which display the vertices where the values of $(x_{i-5},\cdots,x_i,\cdots,x_{i+5})$ satisfy (2) and the directed edges between them in Fig. 4.

As before, this rather dense graph can be simplified by only showing vertices and edges in cycles, as shown in Fig. 5. From this graph, the period-5 points of 3-bit CA Rule 82 can be determined, for example, 00011010100001001011 (complete the cycle following the sequence of vertices: 8, 18, 36, 62, 52, 27, 50, 21, 41, 3, 6, 12, 24, 47, 16, 30, 56, 34, 60, 44) when subject to periodic boundary conditions.

It can be seen from Example 2.1, the cycle graph introduced in this paper is a more straightforward method for identifying periodic points of higher period than 2. Although the computational complexity

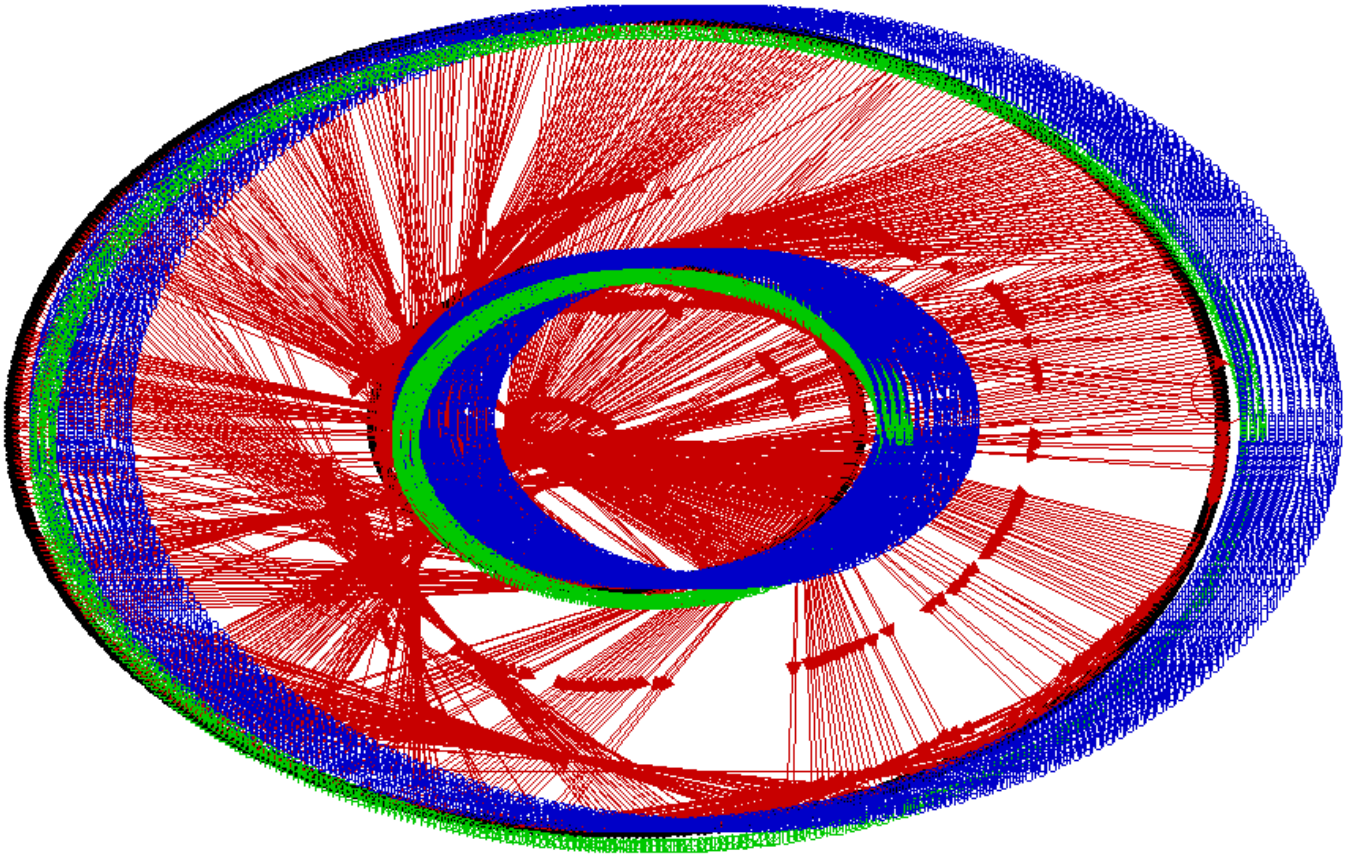

Fig. 4. Directed graph of the 11-bit system.

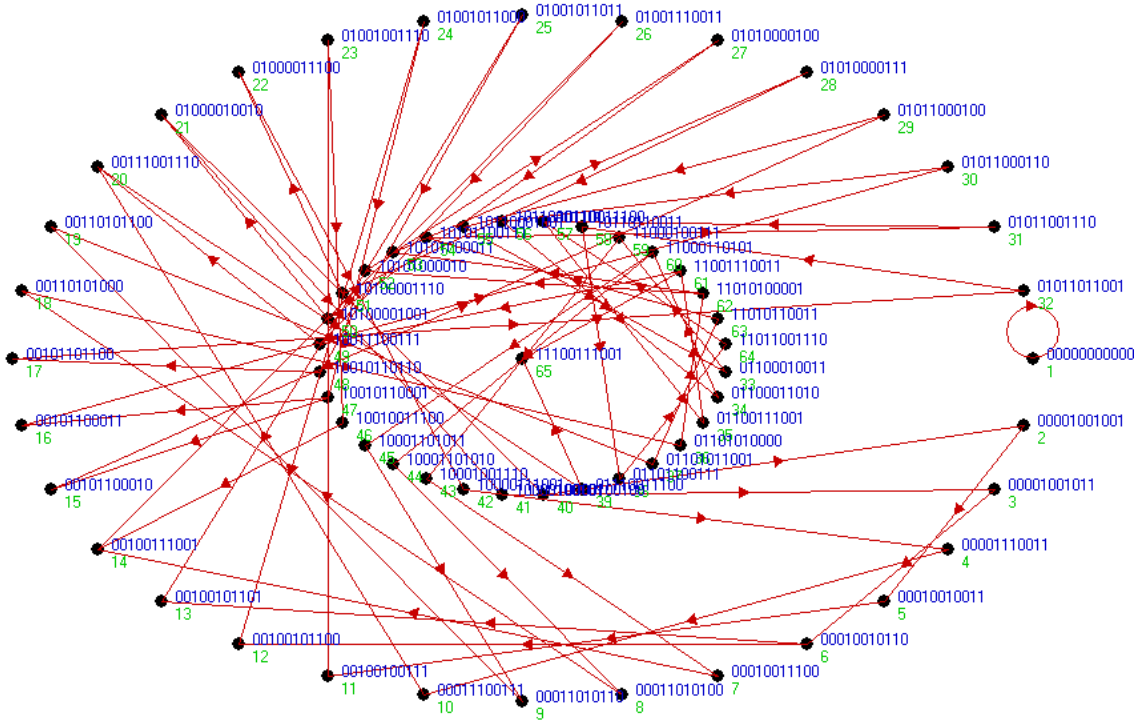

Fig. 5. Simplified directed graph from Fig. 4.

increases when determining periodic points of higher period, in principle, the new cycle graph method works for periodic solutions of any period of 1D CA in general.

Now consider the case of two-dimensional automata. This time we associate two graphs with the system. Again we consider only the numbers of the rule table fixing the mid-point. Rather than considering the general case, we shall simply refer to a 3×3 binary automaton, in order to keep the explanation as simple as possible. (The general case follows easily from the following comments.) Here, we explain the method using a 2D CA with simple rules as an example. Afterwards, we will give another example on a much more complex 2D CA to demonstrate the effectiveness of the method in Example 2.2. For now, consider the (partial) rule table for a simple 3×3 automaton given, in an obvious sense, in Fig. 6 (where a white square corresponds to 0 and a black square to 1).

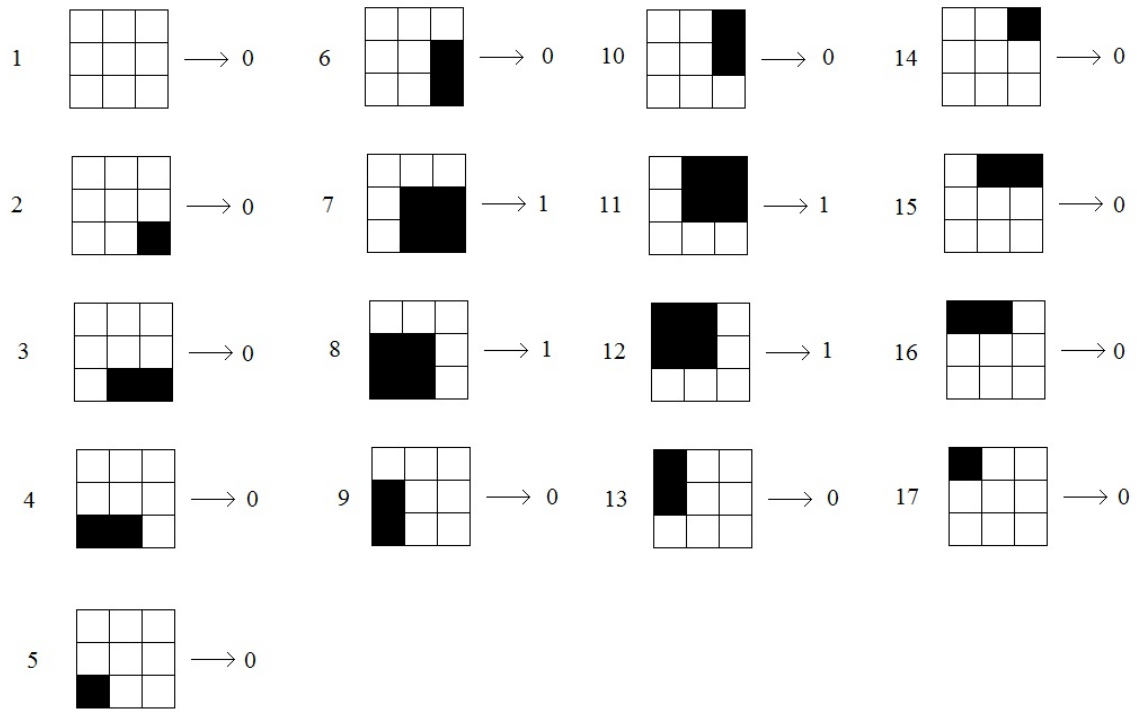

Fig. 6. A partial 3×3 rule table (only the rules fixing the central point are shown).

The graphs associated with the system are as follows: a 'horizontal' graph which has a vertex for each element of the rule table fixing the midpoint. As in the one-dimensional case, a directed edge is drawn from one vertex to another, if the corresponding rule element can be placed together horizontally. Thus, for example, vertices 6 and 7 are connected, since we have the relation as shown in Fig. 7.

We then introduce a 'vertical' graph in a similar way, where vertices can be placed together vertically. We then obtain the two graphs of Fig. 6 as in Fig. 8.

Next we introduce yet another graph from which we may conclude the existence of fixed points. We take the 'horizontal' graph and reduce it to a graph containing only vertices and no edges. This is the 'graph of cycles' of the horizontal graph. In general, there will be an infinite number of cycles in a graph, since we may go around a given cycle any number of times. To obviate this problem we proceed as follows. First we write down all 'prime loops' – i.e. those cycles which contain no other cycles. In Fig. 8, for example, these will be the cycles shown in Fig. 9.

Then we form all cycles which can contain cycles that have already been found. Repeating this procedure, we find all the cycles in which each sub-cycle is only traversed once. Since the original graph is finite, there must be a finite number of such cycles. Again, from Fig. 8, we see that 'second level' cycles are the ones illustrated in Fig. 10.

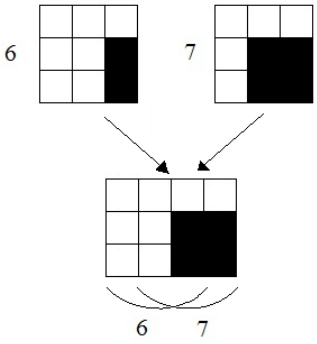

Fig. 7. Horizontal placement of vertices 6 and 7 from Fig. 6.

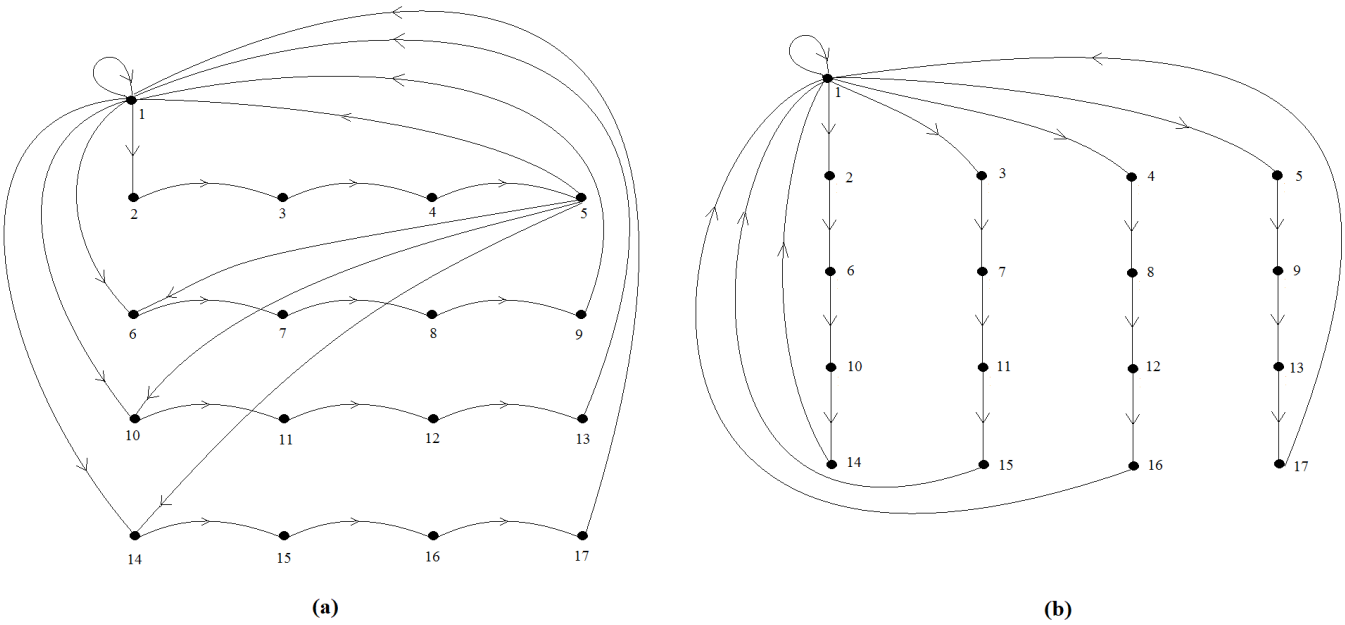

Fig. 8. Graphs for the automaton in Fig. 6. (a) Horizontal graph; (b) Vertical graph.

In this way, we obtain, from the horizontal graph, a finite graph of vertices consisting of its cycles as shown in Fig. 11.

We label these vertices with cycles of integers which correspond to the vertices of the original graph (Fig. 8) which are visited (in order) by these cycles. For example, in Fig. 10, the second level cycle c_{25} is labelled by the cycle

$$(1\ 2\ 3\ 4\ 5\ 1\ 6\ 7\ 8\ 9\ 1).$$

Finally we construct the desired graph (which we call the two-dimensional cycle graph associated with the system) by adding a directed edge from γ_i to γ_j, if we can match the labels of γ_i and γ_j as in Eq. (4):

$$\begin{array}{ll} \gamma_i & (\ m_1 \quad m_2 \ \cdots \ m_k) \\ & \quad \downarrow \quad \downarrow \qquad \downarrow \\ \gamma_j & (\ n_1 \quad n_2 \ \cdots \ n_k), \end{array} \tag{4}$$

where each vertical arrow corresponds to an edge in the 'vertical' graph (we may need to permute γ_i cyclically to do this).

The main result now follows easily from the above remarks: A two-dimensional cellular automaton has a fixed point if and only if its associated two-dimensional cycle graph contains at least one cycle. Note that

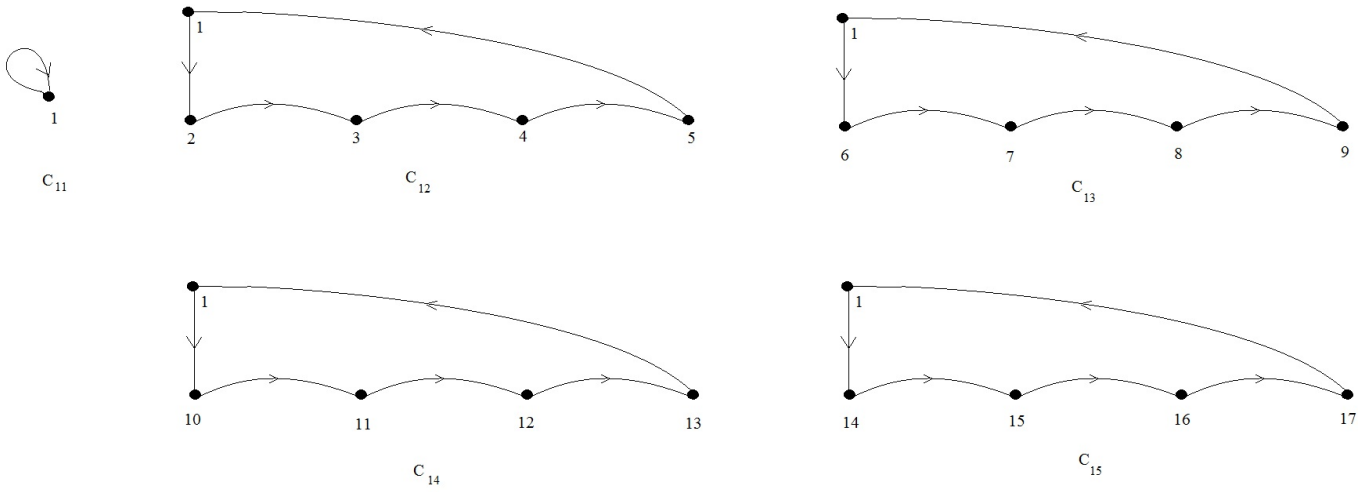

Fig. 9. Prime loops graph cycles of Fig. 8 (a).

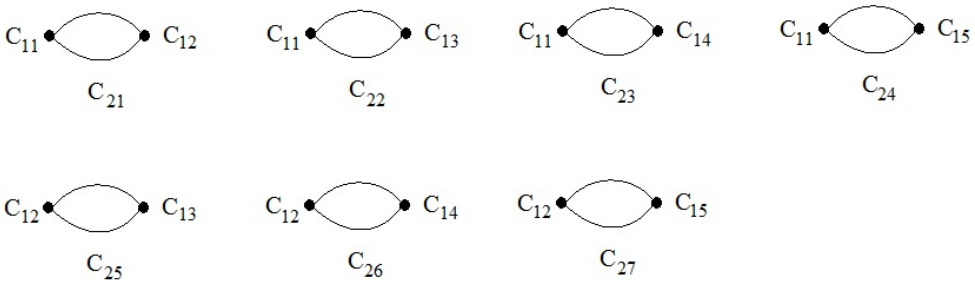

Fig. 10. Second level cycles of Fig. 8.

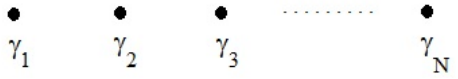

Fig. 11. A finite graph of vertices representing the cycles of Fig. 8.

in the two-dimensional cycle graph we can go round corresponding cycles any number of times. Using this result, we see that the system in Fig. 6 has the fixed points (among others) shown in Fig. 12.

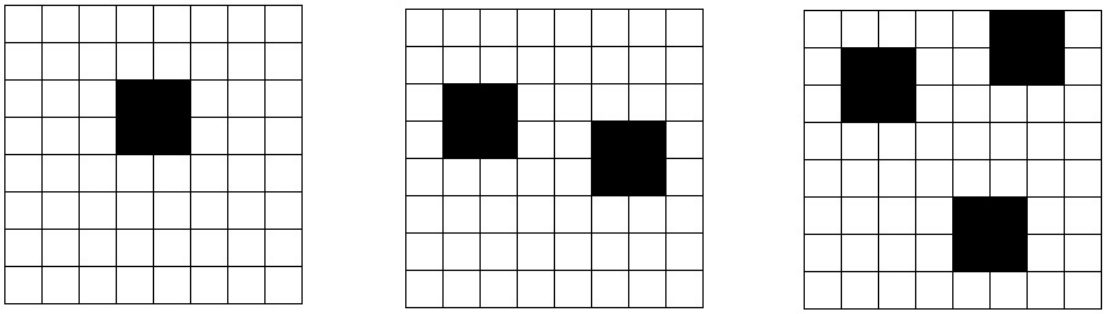

Fig. 12. Fixed points of the 2D CA defined in Fig. 6.

Example 2.2. In this example, we consider a more complex 2D CA – the well-known Conway's game of life [Gardner, 1970], which has the capability of a universal Turing machine [Rendell, 2011]. The system is defined on a 3×3 Moore neighbourhood and the rule table therefore has 512 (2^9) lines, but the evolution rules of this binary CA (1 means 'alive' and 0 means 'dead') can be summarised as follows:

- If the central cell is alive and there are 2 or 3 other alive cells in the neighbourhood, then this central cell will remain alive at the next evolution step; otherwise it will become dead.
- If the central cell is dead and there are exactly 3 alive cells in the neighbourhood, then this central cell will become alive at the next evolution step; otherwise it will remain dead.

The fixed points can be identified using two cycle graphs introduced in this section. Fig. 13 and Fig. 14 below illustrate the 'horizontal' and the 'vertical' graphs, containing a vertex of every configuration in the rule table which fixes the mid-point and directed edges linking vertices when the configurations can be placed together horizontally and vertically, respectively.

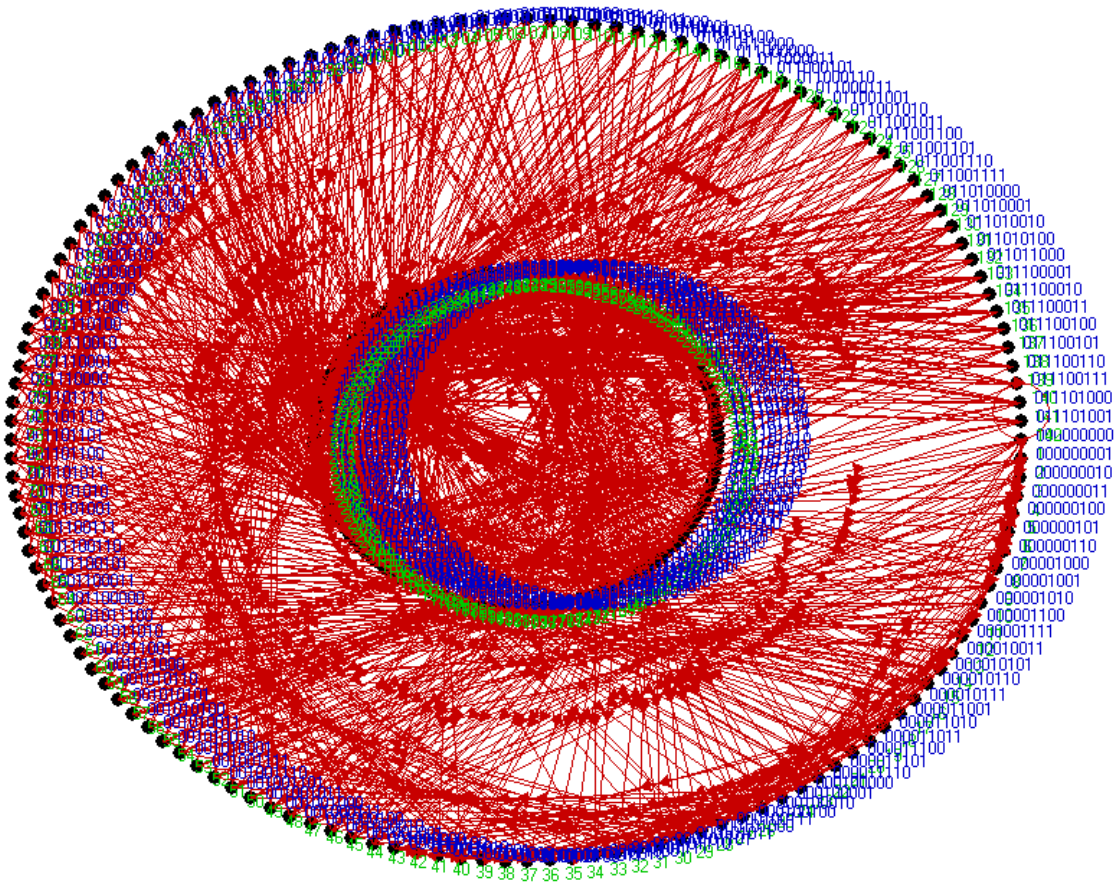

Fig. 13. The horizontal graph for Conway's game of life CA.

Indeed, because of the expected complexity of the dynamics of the game of life CA, these two graphs are very dense. However, fixed points can be identified computationally using algorithms to trace cycles from these horizontal and vertical graphs shown in Fig. 13 and Fig. 14, for example, a fixed point shown in Fig. 15 (where a white square corresponds to 0 and a black square to 1). Note that this 2D CA size is 10×10 and periodic boundary conditions are applied on all sides.

As illustrated in the 1D CA case earlier, periodic points correspond to fixed points of another CA system with a bigger neighbourhood. This theory also extends to 2D CA where periodic solutions can be

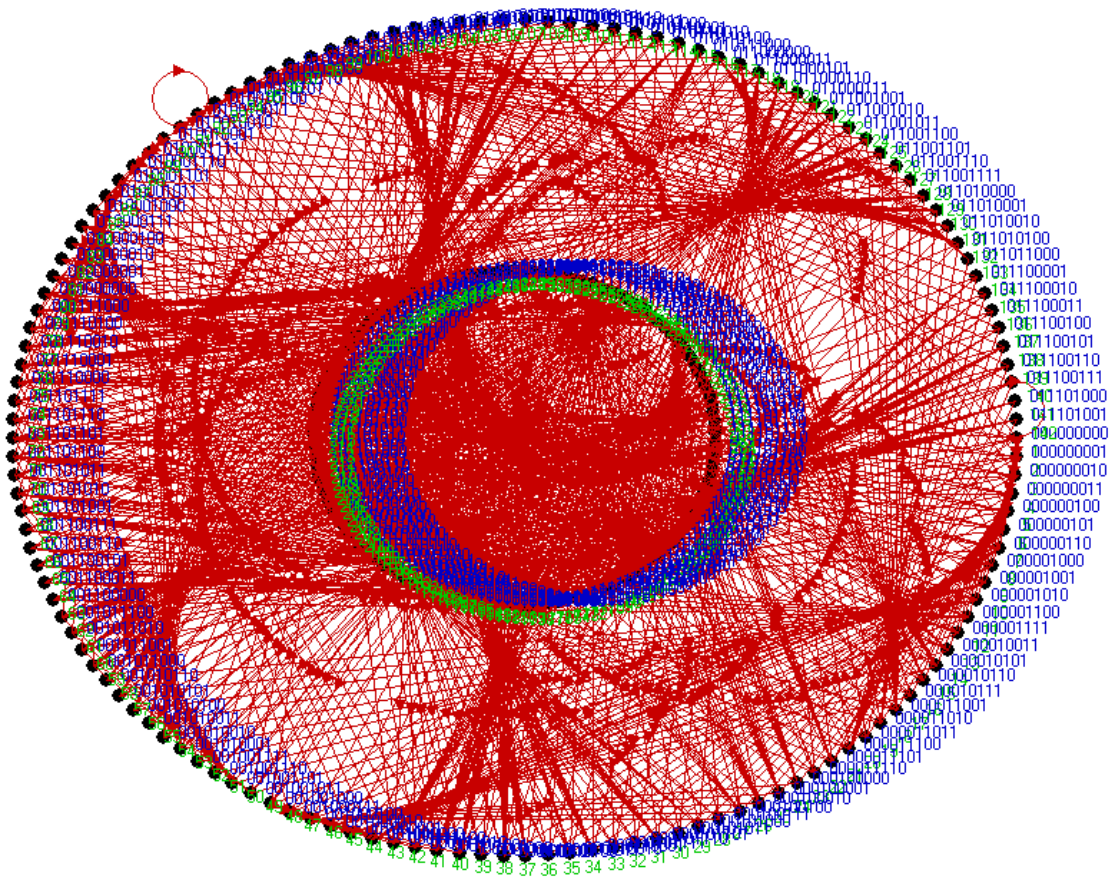

Fig. 14. The vertical graph for Conway's game of life CA.

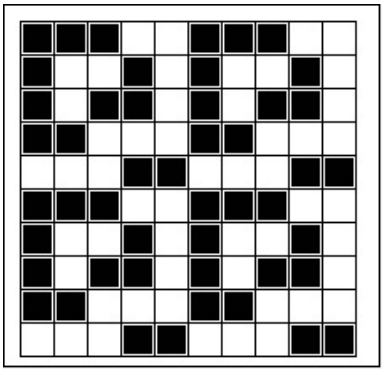

Fig. 15. A fixed point of Conway's game of life CA, identified using the horizontal and vertical graphs.

determined as fixed points of an associated CA with a larger neighbourhood. Although the increase of neighbourhood size poses computational challenges (as the number of entries in the rule table increases dramatically), the cycle graph method presented in this paper is still a valid theoretical technique for finding periodic orbits of high-dimensional CA.

From the discussions in this section, we can see that periodic orbits in most binary automata may be fairly uncommon. This means that the dynamics of such systems may lead to very few 'interesting' features, which are largely determined in dynamical systems by their recurrent behaviour. In contrast to these systems, we shall see in the next sections that real-valued automata can have many periodic

orbits, although, as we shall see next, if strict boundary conditions are imposed it is difficult to find many fixed points. If we remove the boundary conditions and allow infinitely long states then periodic solutions abound. In fact we shall see that such systems have uncountable numbers of periodic solutions of almost arbitrary structure.

3. Equilibria Analysis of Real-Valued Linear Cellular Automata

Recall the definition of 1D p-valued CA from Section 2. Real-valued CA are defined similarly, apart from $x_i \in \mathbb{R}$. Because the local transition functions are now defined on $\mathbb{R}$, unsurprisingly, these automata systems produce far richer behaviours (e.g. hypercyclic or chaotic) than the p-valued systems. In a previous paper [Xu *et al.*, 2011], we demonstrated that even in the cases of linear functions f, i.e.

$$f(x_{i-1}, x_i, x_{i+1}) = \alpha x_{i-1} + \beta x_i + \gamma x_{i+1} \tag{5}$$

where $\alpha, \beta, \gamma \in \mathbb{R}$, the systems still generated a large amount of complex patterns and interesting dynamical behaviours. It was also proven that if $|\gamma| > 1$ and $|\alpha| \cdot |\beta| \cdot |\gamma|$ is small enough, the linear system had dense orbits (or was hypercyclic in the sense of [Bayart and Matheron, 2009]).

Given the fact that even real automata defined by linear rules display a variety of dynamics, it is important to study these automata as dynamical systems, to help understand the relationships between the local governing functions and the corresponding global dynamical behaviours. We start this process with the study of an automaton system's fixed points (or equilibria). In Subsections 3.1 and 3.2, linear automata with two different types of boundary conditions, namely zero and periodic are analysed, respectively. It is shown that the boundary condition of a CA hugely affects its dynamical structure. Subsection 3.3 tackles the situation when the local linear rules are defined on a 5-bit neighbourhood instead of a 3-bit one. The results of fixed points of 5-bit CA can be applied to identify periodic points with period 2 for CA defined on 3-bit neighbourhoods.

3.1. *Zero Boundary Conditions*

When a 1D CA has zero boundary conditions, that means its states $x^{[n]}$ are in the form of

$$\mathbf{x}^{[n]} = (0, 0, \mid x_1^{[n]}, x_2^{[n]}, \cdots, x_m^{[n]}, \mid 0, 0)$$

i.e. the states are bounded by 0s at the two ends. By definition, fixed points of a CA are points which satisfy the following:

$$\mathbf{x}^{[n+1]} = \mathbf{x}^{[n]}$$

for all $n \in \overline{\mathbb{Z}^-}$. For a 3-bit CA, the criterion translates into

$$x_i^{[n+1]} = f(x_{i-1}^{[n]}, x_i^{[n]}, x_{i+1}^{[n]}) = x_i^{[n]},$$

in other words, every value of the next state only depends on the value directly above (at the same position in the state string) in the current state.

It is easily seen from the definition of a fixed point that every system state is a fixed point for a cellular system governed by Eq. (5), where $\alpha = \gamma = 0$ and $\beta = 1$. Next, our study will focus on CA defined by translated linear functions of the form

$$f(x_{i-1}, x_i, x_{i+1}) = a x_{i-1} + (b+1) x_i + c x_{i+1} + d, \tag{6}$$

where $a, b, c, d \in \mathbb{R}$. Note: the new notations a, b and c ($a = \alpha,\ b+1 = \beta,\ c = \gamma$ in Eq. (5).) are for the convenience of calculations and explanation. Fixed points of CA ruled by local functions in Eq. (6) now satisfy:

$$x_i = a x_{i-1} + (b+1) x_i + c x_{i+1} + d,$$

which simplifies to

$$a x_{i-1} + b x_i + c x_{i+1} + d = 0. \tag{7}$$

One standard approach in analysing fixed points is to represent the middle variable x_i in terms of the other ones. This method often encounters difficulties, as at least one other variable in the equation is unknown. However, the zero boundary conditions can be utilised to determine all values of a fixed point as a recurring process if Eq. (7) is considered in the form of

$$x_{i+1} = -\frac{ax_{i-1} + bx_i + d}{c}.$$

Now from left to right, each value of a fixed state can be solved in terms of the ruling function coefficients a, b, c and d. According to the left boundary conditions, $x_{-1} = x_0 = 0$. Therefore:

$$x_1 = -\frac{d}{c}, \tag{8}$$

$$x_2 = -\frac{bx_1 + d}{c} = -\frac{d}{c^2}(-b + c), \tag{9}$$

$$x_3 = -\frac{ax_1 + bx_2 + d}{c} = -\frac{d}{c^3}(b^2 - ac - bc + c^2), \tag{10}$$

$$x_4 = -\frac{ax_2 + bx_3 + d}{c} = -\frac{d}{c^4}(-b^3 + 2abc + b^2c - ac^2 - bc^2 + c^3), \tag{11}$$

$$\vdots \tag{12}$$

$$x_{m-1} = -\frac{ax_{m-3} + bx_{m-2} + d}{c}, \tag{13}$$

$$x_m = -\frac{ax_{m-2} + bx_{m-1} + d}{c}, \tag{14}$$

The boundary conditions on the right hand side implies:

$$x_{m+1} = 0 = -\frac{ax_{m-1} + bx_m + d}{c}, \tag{15}$$

$$x_{m+2} = 0 = -\frac{ax_m + b \cdot 0 + d}{c}. \tag{16}$$

Eq. (16) can be simplified to

$$x_m = -\frac{d}{a}. \tag{17}$$

Furthermore, substitute Eq. (17) into Eq. (15), we obtain

$$x_{m-1} = -\frac{d}{a^2}(a - b). \tag{18}$$

Lemma 1. *Only one fixed point* $\mathbf{x} = (0, 0, | \, 0, 0, \cdots, 0, | \, 0, 0)$ *exists for any zero bounded cellular automaton described by a 3-variable linear function* $f(x_{i-1}, x_i, x_{i+1})$ *in the form of Eq. (5), apart from the case when* $\alpha = \gamma = 0$ *and* $\beta = 1$.

Proof. Eq. (5) is equivalent to Eq. (6) when $d = 0$. d is a common factor in all elements of the fixed point state in Eq.s (8-14), therefore, $d = 0$ leads to every element of the fixed point being 0. ■

The elements x_{m-1} and x_m in Eq. (13) and Eq. (14) must also have d as a common factor, due to the nature of the representations of x_{m-1} and x_m. This eliminates the variable d (where $d \neq 0$) when Eq.s (13) & (18) and Eq.s (14) & (17) are combined to remove x_{m-1} and x_m respectively. Then there are effectively 3 variables a, b & c within 2 simultaneous polynomial equations. These two equations can be solved for any 2 of the variables in terms of the 3rd one to determine the global equilibria of the corresponding real CA systems defined by linear local functions (6).

Remark 3.1. A valid set of a, b, c, d values (where a, b, c cannot all be 0) satisfying Eq.s (13) & (18) and Eq.s (14) & (17) fixes a certain local system function in the form of (6), and also generates a single value for every element of the equilibrium x_1, x_2, $\cdots$ and x_m according to Eq.s (8-14). Therefore, the cellular automaton has only one fixed point, of which values satisfy Eq.s (8-14), including the case when $d = 0$. Systems with any other set of a, b, c, d which do not obey Eq.s (13) & (18) and Eq.s (14) & (17) do not contain fixed points.

Lemma 2. *Any one-dimensional cellular system defined by (6) with zero boundary conditions has no more than 1 equilibrium point.*

Although it can be computationally complicated in practice when the CA size is large, the analytical process described above for determining a cellular system's equilibrium stands for any one-dimensional linear cellular automata (1DLCA) of finite sizes. Next, we present an example of a CA of size 14 to illustrate the fundamental idea, however, as the theory is valid for any finite CA size, the equilibria of CA with lager sizes can be identified using more powerful computers.

Example 3.1. A group of 1D CA governed by local translated linear functions (6) have zero boundary conditions for their states, which are described by

$$\mathbf{x}^{[n]} = (0, 0, \mid x_1^{[n]}, x_2^{[n]}, \cdots, x_{13}^{[n]}, x_{14}^{[n]}, \mid 0, 0). \tag{19}$$

In order to find the CA systems which possess fixed points, the following polynomial equations are to be solved simultaneously:

$$\begin{aligned} x_{13} = & -\tfrac{d}{c^{13}}\big(b^{12} - 11ab^{10}c - b^{11}c + 45a^2b^8c^2 + 10ab^9c^2 + b^{10}c^2 - 84a^3b^6c^3 - 36a^2b^7c^3 - 9ab^8c^3 \\ & -b^9c^3 + 70a^4b^4c^4 + 56a^3b^5c^4 + 28a^2b^6c^4 + 8ab^7c^4 + b^8c^4 - 21a^5b^2c^5 - 35a^4b^3c^5 \\ & -35a^3b^4c^5 - 21a^2b^5c^5 - 7ab^6c^5 - b^7c^5 + a^6c^6 + 6a^5bc^6 + 15a^4b^2c^6 + 20a^3b^3c^6 \\ & +15a^2b^4c^6 + 6ab^5c^6 + b^6c^6 - a^5c^7 - 5a^4bc^7 - 10a^3b^2c^7 - 10a^2b^3c^7 - 5ab^4c^7 - b^5c^7 \\ & +a^4c^8 + 4a^3bc^8 + 6a^2b^2c^8 + 4ab^3c^8 + b^4c^8 - a^3c^9 - 3a^2bc^9 - 3ab^2c^9 - b^3c^9 + a^2c^{10} \\ & +2abc^{10} + b^2c^{10} - ac^{11} - bc^{11} + c^{12}\big) \\ = & \tfrac{d}{a^2}(b - a), \end{aligned} \tag{20}$$

$$\begin{aligned} x_{14} = & -\tfrac{d}{c^{14}}\big(-b^{13} + 12ab^{11}c + b^{12}c - 55a^2b^9c^2 - 11ab^{10}c^2 - b^{11}c^2 + 120a^3b^7c^3 + 45a^2b^8c^3 + 10ab^9c^3 \\ & +b^{10}c^3 - 126a^4b^5c^4 - 84a^3b^6c^4 - 36a^2b^7c^4 - 9ab^8c^4 - b^9c^4 + 56a^5b^3c^5 + 70a^4b^4c^5 \\ & +56a^3b^5c^5 + 28a^2b^6c^5 + 8ab^7c^5 + b^8c^5 - 7a^6bc^6 - 21a^5b^2c^6 - 35a^4b^3c^6 - 35a^3b^4c^6 \\ & -21a^2b^5c^6 - 7ab^6c^6 - b^7c^6 + a^6c^7 + 6a^5bc^7 + 15a^4b^2c^7 + 20a^3b^3c^7 + 15a^2b^4c^7 + 6ab^5c^7 \\ & +b^6c^7 - a^5c^8 - 5a^4bc^8 - 10a^3b^2c^8 - 10a^2b^3c^8 - 5ab^4c^8 - b^5c^8 + a^4c^9 + 4a^3bc^9 \\ & +6a^2b^2c^9 + 4ab^3c^9 + b^4c^9 - a^3c^{10} - 3a^2bc^{10} - 3ab^2c^{10} - b^3c^{10} + a^2c^{11} + 2abc^{11} + b^2c^{11} \\ & -ac^{12} - bc^{12} + c^{13}\big) \\ = & -\tfrac{d}{a}. \end{aligned} \tag{21}$$

Given $a, b, c \in \mathbb{R}$, the numerical solutions of a and c in terms of b are $a = c = -\frac{b}{\sqrt{2}}$. b, d can be any real numbers but 0. For example, let $a = c = -1$, $b = \sqrt{2}$, $d = 1$. Then this 1DLCA is governed by

$$f(x_{i-1}, x_i, x_{i+1}) = -x_{i-1} + (\sqrt{2} + 1)x_i - x_{i+1} + 1. \tag{22}$$

The initial state $\mathbf{x}^{[0]}$ of (19) is specified by Eq.s (8-14):

$$\mathbf{x}^{[0]} = (0,\ 0,\ 1,\ 1+\sqrt{2},\ 2+\sqrt{2},\ 2+\sqrt{2},\ 1+\sqrt{2},\ 1,\ 0,\ 0,\ 1,\ 1+\sqrt{2},\ 2+\sqrt{2},\ 2+\sqrt{2},\ 1+\sqrt{2},\ 1,\ 0,\ 0). \tag{23}$$

Each element of the next state is given by

$$x_i^{[1]} = f(x_{i-1}^{[0]}, x_i^{[0]}, x_{i+1}^{[0]}).$$

Therefore,

$$\mathbf{x}^{[1]} = (0,\ 0,\ 1,\ 1+\sqrt{2},\ 2+\sqrt{2},\ 2+\sqrt{2},\ 1+\sqrt{2},\ 1,\ 0,\ 0,\ 1,\ 1+\sqrt{2},\ 2+\sqrt{2},\ 2+\sqrt{2},\ 1+\sqrt{2},\ 1,\ 0,\ 0) = \mathbf{x}^{[0]}.$$

Obviously, $\mathbf{x}^{[2]} = \mathbf{x}^{[3]} = \mathbf{x}^{[4]} = \cdots = \mathbf{x}^{[n]}$. Hence $\mathbf{x}$ in the form of (23) is one and the only fixed point of the 1DLCA ruled by (22).

Numerical solutions of Eq.s (20, 21) can also be achieved relatively easily if for example, $b = 0$, then we obtain

$$\left\{\{c \to -ia\}, \{c \to ia\}, \{c \to a\}, \left\{c \to -\sqrt[4]{-1}a\right\}, \left\{c \to \sqrt[4]{-1}a\right\}, \left\{c \to -(-1)^{3/4}a\right\}, \left\{c \to (-1)^{3/4}a\right\}\right\}.$$

Similar as earlier, the condition of $a, b, c \in \mathbb{R}$ means $a = c$. In the case of $a = c = \frac{1}{2}$ and $d = 3$, for example, another 1DLCA given by

$$f(x_{i-1}, x_i, x_{i+1}) = \frac{1}{2}x_{i-1} + x_i + \frac{1}{2}x_{i+1} + 3$$

also contains one non-zero equilibrium:

$$\mathbf{x} = (0,\ 0,\ -6,\ -6,\ 0,\ 0,\ -6,\ -6,\ 0,\ 0,\ -6,\ -6,\ 0,\ 0)$$

3.2. *Periodic Boundary Conditions*

A 3-bit 1D CA with periodic boundary conditions implies the system states can be represented by

$$\mathbf{x}^{[n]} = (x_{m-1}^{[n]}, x_m^{[n]}, |\ x_1^{[n]}, x_2^{[n]}, \cdots, x_m^{[n]}, |\ x_1^{[n]}, x_2^{[n]}).$$

We now study the equilibria of 1DLCA without translations. The transition rule is in the general form of

$$f(x_{i-1}, x_i, x_{i+1}) = ax_{i-1} + (b+1)x_i + cx_{i+1}. \tag{24}$$

Fixed points of the 1DLCA satisfy

$$x_i = ax_{i-1} + (b+1)x_i + cx_{i+1},$$

which leads to

$$ax_{i-1} + bx_i + cx_{i+1} = 0.$$

Again, boundary conditions can be used to assist the process of identifying state values of an equilibrium, by represent x_{i+1} in terms of x_{i-1} and x_i:

$$x_{i+1} = -\frac{ax_{i-1} + bx_i}{c}.$$

Values of a fixed point therefore satisfy the following:

$$x_1 = \frac{-bx_m - ax_{m-1}}{c}, \tag{25}$$

$$x_2 = -\frac{ax_m + bx_1}{c} = \frac{(b^2 - ac)x_m + abx_{m-1}}{c^2} \tag{26}$$

$$x_3 = -\frac{ax_1 + bx_2}{c} = \frac{(-b^3 + 2abc)x_m + (-ab^2 + a^2c)x_{m-1}}{c^3} \tag{27}$$

$$x_4 = -\frac{ax_2 + bx_3}{c} = \frac{(b^4 - 3ab^2c + a^2c^2)x_m + (ab^3 - 2a^2bc)x_{m-1}}{c^4} \tag{28}$$

$$\vdots$$

$$x_{m-1} = -\frac{ax_{m-3} + bx_{m-2}}{c}, \tag{29}$$

$$x_m = -\frac{ax_{m-2} + bx_{m-1}}{c}, \tag{30}$$

The boundary conditions on the right hand side are satisfied automatically.

We give an example to explain the details of this method.

Example 3.2. Consider a 1DLCA defined by (24) on a 3-bit neighbourhood of the 10-digit long ($m = 10$) states with periodic boundary conditions. The system states are represented by

$$\mathbf{x}^{[n]} = (x_9^{[n]}, x_{10}^{[n]}, \mid x_1^{[n]}, x_2^{[n]}, \cdots, x_9^{[n]}, x_{10}^{[n]}, \mid x_1^{[n]}, x_2^{[n]}).$$

Elements of fixed solutions of the CA satisfy Eq.s (25-30) when $m = 10$. These equations can be simplified to

$$\begin{array}{c} \alpha x_{10} + \beta x_9 = 0 \\ \gamma x_{10} + \delta x_9 = 0 \end{array}, \tag{31}$$

where $\alpha = b^{10} - 9ab^8c + 28a^2b^6c^2 - 35a^3b^4c^3 + 15a^4b^2c^4 - a^5c^5 - c^{10}$, $\beta = ab^9 - 8a^2b^7c + 21a^3b^5c^2 - 20a^4b^3c^3 + 5a^5bc^4$, $\gamma = -b^9 + 8ab^7c - 21a^2b^5c^2 + 20a^3b^3c^3 - 5a^4bc^4$ and $\delta = -ab^8 + 7a^2b^6c - 15a^3b^4c^2 + 10a^4b^2c^3 - a^5c^4 - c^9$.

Let matrix $A = \begin{pmatrix} \alpha & \beta \\ \gamma & \delta \end{pmatrix}$. When A is invertible, the only set of solutions for (31) is $x_{10} = x_9 = 0$, in which case $x_1 = x_2 = \cdots = x_8 = 0$. The only equilibrium is the all '0' state. When A is singular, however, (31) has many sets of solutions, which indicates many equilibria for a CA system specified by (24). Because $a, b, c \in \mathbb{R}$ and $c \neq 0$, the solutions of $|A| = 0$ are $c = -a - b$ or $c = -a + b$.

When $c = -a - b$, it can be shown that

$$A = \begin{pmatrix} \alpha & -\alpha \\ \frac{\alpha}{a} & -\frac{\alpha}{a} \end{pmatrix} \Rightarrow |A| = 0,$$

where $\alpha = -5a^9b - 20a^8b^2 - 50a^7b^3 - 80a^6b^4 - 86a^5b^5 - 62a^4b^6 - 29a^3b^7 - 8a^2b^8 - ab^9$. Let $a = 1$ and $b = 2$, for example, then $c = -3$. the governing function is

$$f(x_{i-1}, x_i, x_{i+1}) = x_{i-1} + 3x_i - 3x_{i+1}. \tag{32}$$

Eq. (31) in this case becomes

$$\alpha x_{10} - \alpha x_9 = 0.$$

Then any combination of x_9 and x_{10} satisfying $x_9 = x_{10}$ is a valid set of solutions. The number of valid combinations is infinite. If we take $x_9 = 2$ and $x_{10} = 2$, all other values of the initial state can be calculated using Eq.s (25-30). Thus the corresponding fixed point is $(2, 2, \mid 2, 2, 2, 2, 2, 2, 2, 2, 2, 2, \mid 2, 2)$. Indeed, for the 1DLCA defined by (32) with periodic boundary conditions, every point where all the elements equal each other is an equilibrium for this system.

Similar results can be found when $c = -a + b$, which results in

$$A = \begin{pmatrix} \alpha & \alpha \\ -\frac{\alpha}{a} & -\frac{\alpha}{a} \end{pmatrix} \Rightarrow |A| = 0,$$

where $\alpha = 5a^9b - 20a^8b^2 + 50a^7b^3 - 80a^6b^4 + 86a^5b^5 - 62a^4b^6 + 29a^3b^7 - 8a^2b^8 + ab^9$. Again, for any set of a, b, c satisfying $c = -a + b$, it specifies a transition function, which governs a CA with an infinite number of fixed points, where $x_{10} = -x_9$.

Note: The method for finding equilibria detailed above extends to any finite CA sizes.

Remark 3.2. The state $(0, 0, \mid 0, 0, \cdots, 0, \mid 0, 0)$ is always a fixed point of a cellular system governed by (24).

Lemma 3. *The number of equilibria of a one-dimensional cellular automaton given by a linear local rule (24) is either 1 or infinite.*

Lemma 2 and Lemma 3 together demonstrate the important impact boundary conditions have on the equilibria and therefore the dynamical structure of a 1DLCA with finite CA size.

3.3. *5-bit Linear Rules*

As explained in Section 2, periodic solutions of period 2 for the 3-bit automata are fixed points of the equivalent 5-bit automata. Now consider a 1D CA defined on a 5-bit neighbourhood by a translated linear function:

$$f(x_{i-2}, x_{i-1}, x_i, x_{i+1}, x_{i+2}) = ax_{i-2} + bx_{i-1} + (c+1)x_i + dx_{i+1} + ex_{i+2} + g, \tag{33}$$

has system states

$$\mathbf{x}^{[n]} = (0,0,0,0 \mid x_1^{[n]}, x_2^{[n]}, \cdots, x_m^{[n]}, \mid 0,0,0,0).$$

Values of the system's fixed points obey the following condition:

$$ax_{i-2} + bx_{i-1} + cx_i + dx_{i+1} + ex_{i+2} + g = 0.$$

The process of locating fixed points of the system is very similar to the one described in Section 3.1, if the system is bounded by '0s' on both sides of the states. This is achieved by representing x_{i+2} in terms of the other variables, i.e.

$$x_{i+2} = -\frac{ax_{i-2} + bx_{i-1} + cx_i + dx_{i+1} + g}{e}.$$

and using the zero boundary conditions. Although the process of finding elements of fixed states is similar as in Section 3.1, because the CA has a 5-bit local function, the '0's on both sides of the state boundary provide 4 polynomial equations (instead of 2 as of the 3-bit case) by linking x_{m-3}, x_{m-2}, x_{m-1} and x_m, respectively. These 4 new equations contain 5 variables $a,\ b,\ c,\ d$ and e, as g is a common factor which can be eliminated if $g \neq 0$. Numerical solutions of these variables can be calculated to determine the elements of the fixed point of a certain 1DLCA governed by (33). Lemma 2 is also valid for any CA defined by (33).

If a 5-bit 1DLCA has periodic boundary conditions, the system states are in the form of

$$\mathbf{x}^{[n]} = (x_{m-3}^{[n]}, x_{m-2}^{[n]}, x_{m-1}^{[n]}, x_m^{[n]}, \mid x_1^{[n]}, x_2^{[n]}, \cdots, x_m^{[n]}, \mid x_1^{[n]}, x_2^{[n]}, x_3^{[n]}, x_4^{[n]}),$$

and the 5-bit governing function is represented by

$$f(x_{i-2}, x_{i-1}, x_i, x_{i+1}, x_{i+2}) = ax_{i-2} + bx_{i-1} + (c+1)x_i + dx_{i+1} + ex_{i+2}. \tag{34}$$

Similar steps as described in Section 3.2 for determining equilibria can be adopted and A is now a 4×4 matrix. Lemma 3 holds for 1DLCA defined by (34) on a 5-bit neighbourhood.

In the next two sections of the paper, we show that if the state is doubly infinite, so that there are no boundaries, then the system's recurrent behaviour is completely different. In particular, we show that such systems contain uncountably many periodic solutions of all periods.

4. Dynamics of Real Automata

We consider linear dynamics on the infinite-dimensional vector space

$$V = \cdots \oplus \mathbb{R} \oplus \mathbb{R} \oplus \mathbb{R} \oplus \cdots = \bigoplus_{i=-\infty}^{\infty} \mathbb{R}$$

Vectors in this space will be denoted by

$$x = (\cdots,\ x_{-2},\ x_{-1},\ x_0,\ x_1,\ x_2,\ \cdots)^T.$$

We consider first rank 1, 3-bit real automata defined by

$$y = Ax, \tag{35}$$

where A is a doubly-infinite matrix. In terms of coordinates, the dynamics (35) is given by

$$y_i = ax_{i-1} + bx_i + cx_{i+1}, \quad -\infty < i < \infty.$$

Thus, A has the form

$$A = \begin{bmatrix} \ddots & \ddots & \ddots & & & \\ & a & b & c & & \\ & & a & b & c & \\ & & & a & b & c \\ & & & & \ddots & \ddots & \ddots \end{bmatrix},$$

i.e.

$$A = aL_1 + bI + cR_1,$$

where I is the doubly-infinite identity matrix and

$$L_1 = \begin{bmatrix} 0 & & & & \\ 1 & 0 & & \mathbf{0} & \\ & \ddots & \ddots & & \\ & \mathbf{0} & 1 & 0 & \\ & & & 1 & 0 \end{bmatrix}, \quad R_1 = \begin{bmatrix} 0 & 1 & & & \\ & 0 & 1 & \mathbf{0} & \\ & & \ddots & \ddots & \\ & \mathbf{0} & & 0 & 1 \\ & & & & 0 \end{bmatrix}.$$

In order to obtain an explicit form for the dynamics, we introduce the doubly-infinite matrices

$$L_i = (\delta_{k,k-i})_{-\infty<k<\infty}, \; R_i = (\delta_{k,k+i})_{-\infty<k<\infty}.$$

Thus we have

Lemma 4. *The operators L_i, R_i satisfy the relations*

$$R_1 L_1 = L_1 R_1 = I,$$

$$L_i R_j = R_j L_i = \begin{cases} L_{i-j}, & \text{if } i > j \\ I, & \text{if } i = j \\ R_{j-i}, & \text{if } j > i \end{cases},$$

$$\text{and} \quad L_i^k = L_{i\times k}, \quad R_i^k = R_{i\times k} \; .$$

Proof. These follow by elementary computation. (Note, however, that these relations do not hold for finite-dimensional truncations of R_i and L_i.) ■

Theorem 1. *The elements of A^k are given by*

$$\left(A^k\right)_{i,j} = 0, \; \text{if } j < i-k \text{ or } j > i+k,$$

$$\left(A^k\right)_{i,i-l} = \sum_{|p|=k,\; l>0} \frac{k!}{p!} a^{p_1} b^{p_2} c^{p_3}, \; \text{if } \; p_1 - p_3 = l \; \& \; 0 < l \le k,$$

$$\left(A^k\right)_{i,i+l} = \sum_{|p|=k,\; l>0} \frac{k!}{p!} a^{p_1} b^{p_2} c^{p_3}, \; \text{if } \; p_3 - p_1 = l \; \& \; 0 < l \le k,$$

$$\left(A^k\right)_{i,i} = \sum_{|p|=k,\; p_1=p_3} \frac{k!}{p!} a^{p_1} b^{p_2} c^{p_3}.$$

Proof. We have

$$A = aL_1 + bI + cR_1$$

and so

$$\begin{aligned} A^k &= (aL_1 + bI + cR_1)^k \\ &= \sum_{|p|=k} \frac{k!}{p!} \big((aL_1)^{p_1} (bI)^{p_2} (cR_1)^{p_3}\big), \quad \text{(multinomial theorem)} \end{aligned}$$

where $p = (p_1,\ p_2,\ p_3)$ and $p! = p_1!\ p_2!\ p_3!$. Thus, we have

$$\begin{aligned} A^k &= \sum_{|p|=k} \frac{k!}{p!} a^{p_1} b^{p_2} c^{p_3} L_1^{p_1} R_1^{p_3} \\ &= \sum_{|p|=k} \frac{k!}{p!} a^{p_1} b^{p_2} c^{p_3} L_{p_1} R_{p_3} \\ &= \sum_{|p|=k,\ p_1>p_3} \frac{k!}{p!} a^{p_1} b^{p_2} c^{p_3} L_{p_1-p_3} + \sum_{|p|=k,\ p_1=p_3} \frac{k!}{p!} a^{p_1} b^{p_2} c^{p_3} I + \sum_{|p|=k,\ p_1<p_3} \frac{k!}{p!} a^{p_1} b^{p_2} c^{p_3} R_{p_3-p_1}. \end{aligned}$$

Now equate like indices. ■

5. Periodic Solutions of Real Linear Automata

We now consider the periodic points of doubly-infinite real automata. The general state will be denoted by a doubly-infinite vector $x \in \cdots \oplus \mathbb{R} \oplus \mathbb{R} \oplus \mathbb{R} \oplus \cdots$, i.e.

$$x = (\cdots,\ x_{-2},\ x_{-1},\ x_0,\ x_1,\ x_2,\ \cdots)^T.$$

Consider first the case of fixed points, i.e. period 1 orbit. The dynamics are given by

$$y = Ax,$$

or

$$y_i = ax_{i-1} + bx_i + cx_{i+1}, \quad -\infty < i < \infty.$$

For a fixed point we have

$$x_i = ax_{i-1} + bx_i + cx_{i+1}, \quad -\infty < i < \infty,$$

i.e.

$$x_{i+1} = \frac{(1-b)}{c} x_i - \frac{a}{c} x_{i-1}, \quad \forall i \in \mathbb{Z} \tag{36}$$

and

$$x_{i-1} = \frac{(1-b)}{a} x_i - \frac{c}{a} x_{i+1}, \quad \forall i \in \mathbb{Z}. \tag{37}$$

To solve (36), let $s_1 = \frac{1-b}{c}$, $q_1 = -\frac{a}{c}$. Then putting $z_i = \begin{bmatrix} x_{i-1} \\ x_i \end{bmatrix}$, we have

$$z_{i+1} = \begin{bmatrix} 0 & 1 \\ q_1 & s_1 \end{bmatrix} z_i,$$

and so

$$z_i = \begin{bmatrix} 0 & 1 \\ q_1 & s_1 \end{bmatrix}^{i-1} \times z_1 = \begin{bmatrix} 0 & 1 \\ q_1 & s_1 \end{bmatrix}^{i-1} \begin{bmatrix} x_0 \\ x_1 \end{bmatrix}. \tag{38}$$

Similarly, to solve (37), we put $s_2 = \frac{1-b}{a}$, $q_2 = -\frac{c}{a}$ and $z_i = \begin{bmatrix} x_{i+1} \\ x_i \end{bmatrix}$. Then

$$z_{i-1} = \begin{bmatrix} 0 & 1 \\ q_2 & s_2 \end{bmatrix} z_i,$$

and so

$$z_{-i} = \begin{bmatrix} 0 & 1 \\ q_2 & s_2 \end{bmatrix}^i z_0 = \begin{bmatrix} 0 & 1 \\ q_2 & s_2 \end{bmatrix}^i \begin{bmatrix} x_1 \\ x_0 \end{bmatrix}. \tag{39}$$

Hence (38) and (39) give a two-parameter set of fixed points of the dynamical system.

In general, period-k orbits are given by the fixed points of the $(2k+1)$-bit automaton A^k. As above we can write the fixed point equation in the form

$$x_i = \alpha^k_{i,i-k}x_{i-k} + \alpha^k_{i,i-k+1}x_{i-k+1} + \cdots + \alpha^k_{i,i}x_i + \alpha^k_{i,i+1}x_{i+1} + \cdots + \alpha^k_{i,i+k}x_{i+k}.$$

As before we obtain a 'forward' and a 'backward' equation (assuming $\alpha^k_{i,i-k} \neq 0$, $\alpha^k_{i,i+k} \neq 0$):

$$x_{i+k} = \frac{(1-\alpha^k_{i,i})}{\alpha^k_{i,i+k}}x_i - \frac{1}{\alpha^k_{i,i+k}}\left(\alpha^k_{i,i-k}x_{i-k} + \cdots + \alpha^k_{i,i+k-1}x_{i+k-1}\right),$$
$$x_{i-k} = \frac{(1-\alpha^k_{i,i})}{\alpha^k_{i,i-k}}x_i - \frac{1}{\alpha^k_{i,i-k}}\left(\alpha^k_{i,i-k+1}x_{i-k+1} + \cdots + \alpha^k_{i,i+k}x_{i+k}\right).$$

This leads to the equations

$$z_{i+1} = \begin{bmatrix} 0 & 1 & & & \\ & 0 & 1 & & \mathbf{0} \\ \mathbf{0} & & \ddots & \ddots & \\ & & & 0 & 1 \\ q_1^1 & q_1^2 & q_1^3 & \cdots & q_1^{2k} \end{bmatrix} z_i, \tag{40}$$

where $z_i = (x_{i-2k+1}, x_{i-2k+2}, \cdots, x_i)$, and

$$z_{i-1} = \begin{bmatrix} 0 & 1 & & & \\ & 0 & 1 & & \mathbf{0} \\ \mathbf{0} & & \ddots & \ddots & \\ & & & 0 & 1 \\ q_2^1 & q_2^2 & q_2^3 & \cdots & q_2^{2k} \end{bmatrix} z_i, \tag{41}$$

where $z_i = (x_{i+2k-1}, x_{i+2k-2}, \cdots, x_i)$. This gives a $2k$-parameter set of period k points.

Example 5.1. As an example, consider the system given by the infinite matrix A as follows:

$$A = \begin{bmatrix} \ddots & \ddots & \ddots & & & \\ & 0.5 & 0.3 & 0.4 & & \\ & & 0.5 & 0.3 & 0.4 & \\ & & & 0.5 & 0.3 & 0.4 \\ & & & & \ddots & \ddots & \ddots \end{bmatrix},$$

i.e. $a = 0.5$, $b = 0.3$, $c = 0.4$ and $y_i = 0.5x_{i-1} + 0.3x_i + 0.4x_{i+1}$. Then

$$A^2 = \begin{bmatrix} \ddots & \ddots & \ddots & \ddots & \ddots & & & \\ & 0.25 & 0.3 & 0.49 & 0.24 & 0.16 & & \\ & & 0.25 & 0.3 & 0.49 & 0.24 & 0.16 & \\ & & & 0.25 & 0.3 & 0.49 & 0.24 & 0.16 \\ & & & & \ddots & \ddots & \ddots & \ddots & \ddots \end{bmatrix},$$

Solving Equations (40) and (41), we find the period-2 point:

$$(\cdots, 15.747, -7.4434, 3.0464, -1.292, 1, 0.3, 0.4, 0.5, -1.6, 2.775, -10.825, 27.302, \cdots)^T.$$

6. Conclusions

In this paper, a previously discovered graph theory based technique [Xu *et al.*, 2009] for finding period solutions of one-dimensional binary automata has been extended to two-dimensional and p-valued CA. We have demonstrated the effectiveness of this approach in the binary situations, where periodic orbits

are uncommon and difficult to identify traditionally. The rich dynamical behaviours of cellular systems based on real-valued states have also been studied. We have shown that boundary conditions play very important roles in the dynamical structure of cellular systems. As shown in this paper, when strict boundary conditions are imposed, fixed points and periodic solutions are very much restricted. However, when the boundary conditions are relaxed and the system is defined on infinite-dimensional vector space, there exist uncountable numbers of periodic orbits of almost arbitrary structure. Including boundary conditions (even for linear systems) introduces high order polynomial equations, as shown in Examples 3.1 and 3.2. Whatever approach is taken, these equations will have to be solved, to identify periodic points. In a forthcoming paper, we shall show how to deal with general boundary conditions in both 1D and 2D linear CA.

The findings presented in this paper lead to better understanding of cellular systems' dynamics when CA are used as a modelling tool in a variety of applications. In particular, our future research will focus on the dynamics of two- and three-dimensional lattice gas cellular automata and lattice Boltzmann models [Halliday *et al.*, 2017], [Xu *et al.*, 2017], where real-valued states are adopted. Note finally, that the methods of Section 5 can be applied to nonlinear systems, by using the implicit function theorem, although we can no longer obtain explicit solutions as in Section 4.

Acknowledgement

The author would like to thank Emeritus Professor Prof. Stephen Paul Banks from the University of Sheffield (UK) for his helpful advice on the research work in this paper. The author is very grateful to his support and guidance.

References

Al-Husari, M., Murdoch, C. & Webb, S. D. [2014] "A cellular automaton model examining the effects of oxygen, hydrogen ions and lactate on early tumour growth," *Journal of mathematical biology* **69**, 839–873.

Avolio, M. V., Di Gregorio, S., Lupiano, V. & Mazzanti, P. [2013] "Sciddica-ss 3: a new version of cellular automata model for simulating fast moving landslides," *The Journal of Supercomputing* **65**, 682–696.

Bayart, F. & Matheron, É. [2009] *Dynamics of linear operators*, Vol. 179 (Cambridge university press).

Beauchemin, C., Samuel, J. & Tuszynski, J. [2005] "A simple cellular automaton model for influenza a viral infections," *Journal of theoretical biology* **232**, 223–234.

Bhattacharjee, K., Das, S. *et al.* [2018] "A list of tri-state cellular automata which are potential pseudo-random number generators," *International Journal of Modern Physics C (IJMPC)* **29**, 1–35.

Bhattacharjee, K., Naskar, N., Roy, S. & Das, S. [2016] "A survey of cellular automata: Types, dynamics, non-uniformity and applications," *arXiv preprint arXiv:1607.02291* .

Bossomaier, T. R. & Green, D. G. [2000] *Complex systems* (Cambridge university press).

Burkhead, E. & Hawkins, J. [2015] "A cellular automata model of ebola virus dynamics," *Physica A: Statistical Mechanics and its Applications* **438**, 424–435.

Chopard, B. [2012] "Cellular automata and lattice boltzmann modeling of physical systems," *Handbook of Natural Computing* (Springer), pp. 287–331.

Chopard, B. & Droz, M. [1998] *Cellular automata* (Springer).

Chopard, B., Dupuis, A., Masselot, A. & Luthi, P. [2002] "Cellular automata and lattice boltzmann techniques: An approach to model and simulate complex systems," *Advances in complex systems* **5**, 103–246.

Chopard, B. & Masselot, A. [1999] "Cellular automata and lattice boltzmann methods: a new approach to computational fluid dynamics and particle transport," *Future Generation Computer Systems* **16**, 249–257.

Chua, L. O., Guan, J., Sbitnev, V. I. & Shin, J. [2007a] "a nonlinear dynamics perspective of wolfram's new kind of science part vii: Isles of eden," *International Journal of Bifurcation and Chaos* **17**, 2839–3012.

Chua, L. O., Karacs, K., Sbitnev, V. I., Guan, J. & Shin, J. [2007b] "a nonlinear dynamics perspective of wolfram's new kind of science part viii: More isles of eden," *International Journal of Bifurcation and Chaos* **17**, 3741–3894.

Chua, L. O., Pazienza, G. E., Orzó, L., Sbitnev, V. I. & Shin, J. [2008] "a nonlinear dynamics perspective of wolfram's new kind of science part ix: Quasi-ergodicity," *International Journal of Bifurcation and Chaos* **18**, 2487–2642.

Chua, L. O., Sbitnev, V. I. & Yoon, S. [2003] "A nonlinear dynamics perspective of wolfram's new kind of science part ii: Universal neuron," *International Journal of Bifurcation and Chaos* **13**, 2377–2491.

Chua, L. O., Sbitnev, V. I. & Yoon, S. [2004] "a nonlinear dynamics perspective of wolfram's new kind of science part iii: Predicting the unpredictable," *International Journal of Bifurcation and Chaos* **14**, 3689–3820.

Chua, L. O., Sbitnev, V. I. & Yoon, S. [2005a] "a nonlinear dynamics perspective of wolfram's new kind of science part iv: from bernoulli shift to 1/f spectrum," *International Journal of Bifurcation and Chaos* **15**, 1045–1183.

Chua, L. O., Sbitnev, V. I. & Yoon, S. [2005b] "a nonlinear dynamics perspective of wolfram's new kind of science part v: Fractals everywhere," *International Journal of Bifurcation and Chaos* **15**, 3701–3849.

Chua, L. O., Sbitnev, V. I. & Yoon, S. [2006] "a nonlinear dynamics perspective of wolfram's new kind of science part vi: from time-reversible attractors to the arrow of time," *International Journal of Bifurcation and Chaos* **16**, 1097–1373.

Chua, L. O., Yoon, S. & Dogaru, R. [2002] "A nonlinear dynamics perspective of wolfram's new kind of science part i: Threshold of complexity," *International Journal of Bifurcation and Chaos* **12**, 2655–2766.

Dabbaghian, V., Jackson, P., Spicer, V. & Wuschke, K. [2010] "A cellular automata model on residential migration in response to neighborhood social dynamics," *Mathematical and Computer Modelling* **52**, 1752–1762.

Ermentrout, G. B., Edelstein-Keshet, L. *et al.* [1993] "Cellular automata approaches to biological modeling," *Journal of theoretical Biology* **160**, 97–133.

Frisch, U., Hasslacher, B. & Pomeau, Y. [1986] "Lattice-gas automata for the navier-stokes equation," *Physical review letters* **56**, 1505.

Gardner, M. [1970] "Mathematical games: The fantastic combinations of john conways new solitaire game life," *Scientific American* **223**, 120–123.

Halliday, I., Xu, X. & Burgin, K. [2017] "Shear viscosity of a two-dimensional emulsion of drops using a multiple-relaxation-time-step lattice boltzmann method," *Physical Review E* **95**, 023301.

Han, F., Tang, B., Kou, H., Li, J. & Feng, Y. [2015] "Cellular automata simulations of grain growth in the presence of second-phase particles," *Modelling and Simulation in Materials Science and Engineering* **23**, 065010.

Ilachinski, A. [2001] *Cellular automata: a discrete universe* (World Scientific Publishing Company).

Jen, E. [1989] "Enumeration of preimages in cellular automata," *Complex Systems* **3**, 421–456.

Karafyllidis, I. & Thanailakis, A. [1997] "A model for predicting forest fire spreading using cellular automata," *Ecological Modelling* **99**, 87–97.

Liu, Y., Hu, Y., Long, S., Liu, L. & Liu, X. [2017] "Analysis of the effectiveness of urban land-use-change models based on the measurement of spatio-temporal, dynamic urban growth: A cellular automata case study," *Sustainability* **9**, 796.

Machicao, J., Marco, A. G. & Bruno, O. M. [2012] "Chaotic encryption method based on life-like cellular automata," *Expert Systems with Applications* **39**, 12626–12635.

Mainzer, K. & Chua, L. [2011] *The universe as automaton: From simplicity and symmetry to complexity*, Vol. 1 (Springer Science & Business Media).

Martinez, G. J. [2013] "A note on elementary cellular automata classification," *arXiv preprint arXiv:1306.5577* .

Martínez, G. J., Adamatzky, A., Chen, B., Chen, F. & Seck-Tuoh-Mora, J. C. [2018] "Simple networks on complex cellular automata: From de bruijn diagrams to jump-graphs," *Evolutionary Algorithms, Swarm Dynamics and Complex Networks* (Springer), pp. 241–264.

McIntosh, H. V. [1991] "Linear cellular automata via de bruijn diagrams," *preprint, May* .

McIntosh, H. V. [2009] *One dimensional cellular automata* (Luniver Press).

McIntosh, H. V. [2010] "Lifes still lifes," *Game of Life Cellular Automata* (Springer), pp. 35–50.

Perez, L. & Dragicevic, S. [2012] "Landscape-level simulation of forest insect disturbance: Coupling swarm intelligent agents with gis-based cellular automata model," *Ecological modelling* **231**, 53–64.

Ping, P., Xu, F. & Wang, Z.-J. [2014] "Image encryption based on non-affine and balanced cellular automata," *Signal Processing* **105**, 419–429.

Powathil, G. G., Gordon, K. E., Hill, L. A. & Chaplain, M. A. [2012] "Modelling the effects of cell-cycle heterogeneity on the response of a solid tumour to chemotherapy: biological insights from a hybrid multiscale cellular automaton model," *Journal of theoretical biology* **308**, 1–19.

Raabe, D. [2002] "Cellular automata in materials science with particular reference to recrystallization simulation," *Annual review of materials research* **32**, 53–76.

Rai, A., Markl, M. & Körner, C. [2016] "A coupled cellular automaton–lattice boltzmann model for grain structure simulation during additive manufacturing," *Computational Materials Science* **124**, 37–48.

Rendell, P. [2011] "A universal turing machine in conway's game of life," *High Performance Computing and Simulation (HPCS), 2011 International Conference on* (IEEE), pp. 764–772.

Sahin, U., Uguz, S. & Akin, H. [2015] "The transition rules of 2d linear cellular automata over ternary field and self-replicating patterns," *International Journal of Bifurcation and Chaos* **25**, 1550011.

Sutner, K. [1991] "De bruijn graphs and linear cellular automata," *Complex Systems* **5**, 19–30.

Svyetlichnyy, D. S. [2012] "Simulation of microstructure evolution during shape rolling with the use of frontal cellular automata," *ISIJ international* **52**, 559–568.

Uguz, S., Akin, H. & Siap, I. [2013] "Reversibility algorithms for 3-state hexagonal cellular automata with periodic boundaries," *International Journal of Bifurcation and Chaos* **23**, 1350101.

Uguz, S., Redjepov, S., Acar, E. & Akin, H. [2017] "Structure and reversibility of 2d von neumann cellular automata over triangular lattice," *International Journal of Bifurcation and Chaos* **27**, 1750083.

Vertyagina, Y. & Mahfouf, M. [2015] "A 3d cellular automata model of the abnormal grain growth in austenite," *Journal of materials science* **50**, 745–754.

Vertyagina, Y., Mahfouf, M. & Xu, X. [2013] "3d modelling of ferrite and austenite grain coarsening using real-valued cellular automata based on transition function," *Journal of Materials Science* **48**, 5517–5527.

Von Neumann, J., Burks, A. W. *et al.* [1966] "Theory of self-reproducing automata," *IEEE Transactions on Neural Networks* **5**, 3–14.

Voorhees, B. H. [1996] *Computational analysis of one-dimensional cellular automata*, Vol. 15 (World Scientific).

Wang, M., Zhou, J., Yin, Y., Nan, H., Zhang, D. & Tu, Z. [2017] "A three-dimensional cellular automata model coupling energy and curvature-driven mechanisms for austenitic grain growth," *Metallurgical and Materials Transactions B* **48**, 2245–2255.

Wolf-Gladrow, D. A. [2004] *Lattice-gas cellular automata and lattice Boltzmann models: an introduction* (Springer).

Wolfram, S. [1984] "Universality and complexity in cellular automata," *Physica D: Nonlinear Phenomena* **10**, 1–35.

Wolfram, S. [2018] *Cellular automata and complexity: collected papers* (CRC Press).

Wuensche, A. [1992] "Basins of attraction in disordered networks," *Artificial Neural Networks, 1992* (Elsevier), pp. 1325–1330.

Wuensche, A. [2000] "Basins of attraction in cellular automata," *Complexity* **5**, 19–25.

Wuensche, A. [2017] "Basins of attraction of cellular automata and discrete dynamical networks," *Encyclopedia of Complexity and Systems Science* , 1–16.

Wuensche, A. & Lesser, M. [1992] *Global Dynamics Of Cellular Automata: An Atlas Of Basin Of Attraction Fields Of One-dimensional Cellular Automata*, 1 (Andrew Wuensche).

Xiao, X., Shao, S.-H. & Chou, K.-C. [2006] "A probability cellular automaton model for hepatitis b viral infections," *Biochemical and biophysical research communications* **342**, 605–610.

Xu, X., Banks, S. P. & Mahfouf, M. [2011] "On the structure of real-valued one-dimensional cellular automata," *International Journal of Bifurcation and Chaos* **21**, 1265–1279.

Xu, X., Burgin, K., Ellis, M. & Halliday, I. [2017] "Benchmarking of three-dimensional multicomponent lattice boltzmann equation," *Physical Review E* **96**, 053308.

Xu, X., Song, Y. & Banks, S. P. [2009] "On the dynamical behavior of cellular automata," *International Journal of Bifurcation and Chaos* **19**, 1147–1156.

Zhao, Y., Qin, R. & Chen, D. [2013] "A three-dimensional cellular automata model coupled with finite element method and thermodynamic database for alloy solidification," *Journal of Crystal Growth* **377**, 72–77.

Zhu, B., Zhang, Y., Wang, C., Liu, P. X., Liang, W. K. & Li, J. [2014] "Modeling of the austenitization of ultra-high strength steel with cellular automation method," *Metallurgical and Materials Transactions A* **45**, 3161–3171.